Microchim Acta (2017) 184:3681–3687
DOI 10.1007/s00604-017-2382-1

ORIGINAL PAPER

A zinc(II) benzenetricarboxylate metal organic framework with unusual adsorption properties, and its application to the preconcentration of pesticides

Xuemei Wang[1,2] · Xiaomin Ma[1] · Huan Wang[1] · Pengfei Huang[1] · Xinzhen Du[1,2] · Xiaoquan Lu[1,2]

Received: 20 March 2017 / Accepted: 13 June 2017 / Published online: 3 July 2017

Abstract The authors describe a zinc(II) benzenetricarboxylate (Zn-BTC) based metal-organic framework (MOF) with chrysanthemum-like structure, and its application to the adsorption of pesticides from real water samples. The Zn-BTC MOF was characterized by XRD, TGA, SEM, nitrogen adsorption-desorption analysis and FT-IR spectroscopy. The MOF was used in dispersive solid-phase extraction of six aromatic pesticides from various wastewater samples prior to their quantification by HPLC. Extraction times, extraction temperature, amount of adsorbent, and oscillation rate were optimized. Under the optimal conditions, the method has relative standard deviations (RSDs) of 6.1–10.1%, and good linearity (correlation coefficients higher than 0.9974). The LODs and LOQs for seven pesticides are found to be 0.20–1.60 μg·L^{-1} and 0.66–5.28 μg·L^{-1}, respectively. The RSDs of within batch extraction are 1.6–9.5% and 3.9–12%.

Keywords Dispersive solid-phase extraction · High performance liquid chromatography · SEM · Nitrogen adsorption-desorption · Water analysis · Environmental analysis

Electronic supplementary material The online version of this article (doi:10.1007/s00604-017-2382-1) contains supplementary material, which is available to authorized users.

✉ Xuemei Wang
wxm98@163.com

[1] College of Chemistry and Chemical Engineering, Northwest Normal University, Lanzhou, China

[2] Key Laboratory of Bioelectrochemistry & Environmental Analysis of Gansu Province, Lanzhou 730070, China

Introduction

Metal-organic frameworks (MOFs), known as metal organic coordination polymers, commonly recognized as "soft" analogues of zeolites, is a new class of porous and crystalline materials [1, 2]. The assembly of MOFs constructed from metal ions or metal ion clusters as connectors and organic ligands as linkers, which have attracted considerable attention over the past decade, owing to their enormous varieties of interesting diverse topology and wide potential applications as functional materials, such as hydrogen storage, gas separation, catalysis, sensing, and imaging due to their large surface area, high thermal stability, tunable pore size and other merits [3–8]. All of these applications bring with them a clear and persistent need for increasing control over the properties of MOFs, including crystal size [9, 10], crystal morphology [11, 12] and chemical composition and structure [13–15].

At present, there are many techniques for realizing synthetic control over the properties of MOFs. One or two dimensional nanostructures, such as nanorods and nanosheets can be directly produced following an original crystal structure of target materials in chemical solution systems [16, 17]. Moreover, the addition of a certain kind of modification agent to solutions can tailor the morphology of materials in a desired manner [18, 19]. The approaches can be broadly classified as either modification of a stable final MOF structure or change of synthetic conditions. However, a drastic morphological change both in size and in shape is difficult to achieve because the original crystal structure is being defined in the respective materials. Some studies have demonstrated that self-template method for directing the morphology of nanostructured materials, thus, a new MOF structures and morphologies was gotten, apart from the crystal structure of the objective metal oxide, with an appropriate choice of intermediate compounds

[20]. The structural diversity of MOFs can proceed through several metastable intermediate structures [21].

In the present work, we describe the synthesis and characteristics of different Zn-BTC (BTC = 1,3,5-benzenetricarboxylate) based-MOFs by solvent thermal method, direct addition method and diffusion technique, with respect of morphology, choice of expansion reagent (cyclohexane) and change of solvent allows for anisotropic growth of MOFs, which enables the synthesis of various shapes of Zn-BTC. Because MOFs have received much attentions for gas adsorption application, however, there are limited information about their liquid adsorption properties, for this purpose, the adsorption properties of Zn-BTC as adsorbent of dispersive solid phase extraction (DSPE) combined with HPLC were investigated. Remarkably, the Zn-BTC demonstrated significant adsorption properties for six pesticides removal.

Materials and methods

Materials and chemicals

Pesticides standards containing Avermectin, Pyridaben, Dursban, Carbofuran Fenvalerate and Triadimefon were acquired from National Institute of Metrology (Beijing, China, http://www.nim.ac.cn/), the structures of six pesticides were given in Table S1. Zinc Chloride ($ZnCl_2$), 1,3,5-benzenetricarboxylic acid (H_3BTC), N,N-dimethylformamide (DMF), cyclohexane, and triethylamine were from Rionlon Bohua (Tianjin) Pharmaceutical & Chemical Co. Ltd. (China, http://www.rionlon.com/comcontent_detail01/i=5&comContentId=5.html) and used directly without further purification. Methanol and anhydrous ethanol were from (Fisher Scientific, China, http://www.fishersci.com.cn/v2/). All used deionized water in the experiment was prepared by Aquapro Water Purification System (Chongqing, China, http://cqyiyang.bioon.com.cn/).

The stock solutions of 100 $mg{\cdot}L^{-1}$ each pesticide was prepared in deionized water and stored in amber bottles in the refrigerator at 4 °C. The standard working solutions were prepared by diluting the stock solution with deionized water to the required concentration. Two real water samples were collected from the East River (Industrial wastewater) and West River (Domestic sewage) (Baiyin, Gansu Province, China). Tap water was from our lab. All these samples were filtrated through 0.45 μm glass fiber membrane (Automatic Science, China) and stored in brown glass bottles at 4 °C.

Instrument and chromatographic conditions

FT-IR spectra were recorded on a Digilab FTS3000 FTIR spectrometer using the KBr wafer technique. Thermal gravimetric analysis (TGA) was performed using a TGA 2050 with a ramping rate of 5 $°C{\cdot}min^{-1}$ from 25 to 800 °C under air. The XRD measurements were carried out on a D/max-2400 X-ray powder diffractometer (Japan, Rigaku), using CuKα radiation (40 kV, 30 mA) source with a resolution of 0.02° and scanning speed of 0.5 $°{\cdot}min^{-1}$. SEM images were recorded on a ULTRA Plus (Germany Zeiss). TEM were conducted on Tecnai G2 F20 (FEI, USA) with an accelerating voltage of 80 kV was used. Nitrogen adsorption-desorption isotherms were performed at 77 K on a Quantachrome AS1Win™. The specific surface area was calculated from the adsorption-desorption isotherm by using the Brunauer-Emmet-Teller (BET) equation and the pore size was calculated from the adsorption isotherm by applying the Barret-Joyner-Halenda (BJH) method. Oscillation in extraction procedure was performed by a SHZ-82A environmental incubator shaker (Changzhou Guohua Electric Co., Ltd., China).

The Agilent 1260 series HPLC-UV system (Agilent Technologies, USA) with a variable wavelength detector and a reverse phase C_{18} HPLC column (5 μm, 150 mm × 4.6 mm, Agilent, USA) were used for quantitative analysis. Mobile phase flow rate was 1.0 $mL{\cdot}min^{-1}$ and was constituted of the organic phase A (methanol) and aqueous solution B (water), (A/B = 90:10, *v*/v). The wavelength of UV detection was 230 nm and the sample injection volume was 20 μL.

Assembly procedure

The Zn-BTC MOFs was synthesized by direct addition method, diffusion technique, and solvent thermal method, respectively. (1) Direct addition method, a mixture of H_3BTC (0.06 g) and $ZnCl_2$ (0.30 g) were dissolved in triethylamine (0.5 mL) and DMF (10 mL), and diluted with distilled water (3 mL). Then triethylamine (0.05 mL) was allowed to diffuse slowly into the original mixture. Afterwards, these mixture were sealed with a sealing film and placed in an oven at 80 °C. After 8 h, colorless crystals were filtrated from the resulting solution and washed three times using DMF, and natural drying. The end products were labeled as Zn-BTC-A. (2) Diffusion method, H_3BTC (0.1 mmol) and $ZnCl_2$ (0.2 mmol) was dissolved in DMF (10 mL) and cyclohexane (1 mL) in 25 mL small beaker at room temperature. A mixture of triethylamine (0.5 mL) and DMF (5.0 mL) was placed in 100 mL big beaker. Then the small beaker was placed in big beaker, the big beaker was sealed with a sealing film and maintained for 14 h in an oven at 80 °C, and then white floccules were appeared. The product were filtrated and washed three times with DMF, and then dried under vacuum at 60 °C and used for further experiments. The finished products were labeled as Zn-BTC-D. In order to compare, the other

sample was prepare using same diffusion technique without the addition of cyclohexane, which was labeled as Zn-BTC-D (No cyclohexane). (3) Solvothermal method, an original mixture were prepared by direct addition method, then the mixture was transferred into a Teflon-lined autoclave and heated at 80 °C. After 10 h, colorless crystals were filtrated from the resulting solution and washed three times with DMF, and natural drying. The achieved products were labeled as Zn-BTC-S.

Procedure of adsorption and separation

For preconcentration of pesticide, 10 mg of Zn-BTC was dispersed in 15 mL of sample solution in centrifuge tube, then the sample solution was shaken in oscillator with 200 rpm and at 25 °C. After 30 min, Zn-BTC was separated in centrifuge for 5.0 min with 5000 rpm, and then 20 μL of upper solution was taken and injected into HPLC and used to analyze the residual concentrations of pesticides in sample. The equilibrium adsorption capacity q_e ($\mu g \cdot g^{-1}$) was calculated according to Eq. (1):

$$qe = \frac{(C_0 - C_e) \times V}{m} \quad (1)$$

where C_0 and C_e are the initial and final concentrations ($\mu g \cdot L^{-1}$) of pesticides in sample solution, respectively, V (L) is the volume of the sample solution, and m (g) is the mass of adsorbent.

Results and discussion

Choice of materials

Adsorption is a separation technology with a great potential for reducing energy consumption. The primary requirement in any adsorption process is to choose an adsorption material with high selectivity, capacity and life. To date, several MOFs including IRMOFs, ZIFs and MILs have been used as adsorbent for enrichment and preconcentration of various analytes. More and more researchers have focused their attention on the rational design and optimization of novel MOFs. By varying inorganic/organic components, molecular topologies and organic linkers, ideally novel MOFs with additional features can be created [22]. Herein, with the help of design of task-specific adsorbents, the new MOFs are believed to have superior potential for adsorption applications.

Characterization of Zn-BTC MOFs

Figure 1a shows the FT-IR spectra of Zn-BTC-D (The FT-IR spectra of Zn-BTC-A and Zn-BTC-S are same as Zn-BTC-D). The main functional groups of the predicted structure can be observed with corresponding infrared absorption peaks. The absence of peaks at 1720–1680 cm^{-1} suggested that deprotonation has happened in acidic COOH, which clearly indicate that the carboxylate ion participates in the complex formation. The characteristic vibration at 754 cm^{-1} may be attributed to Zn-O stretching vibration, in which the oxygen atom is

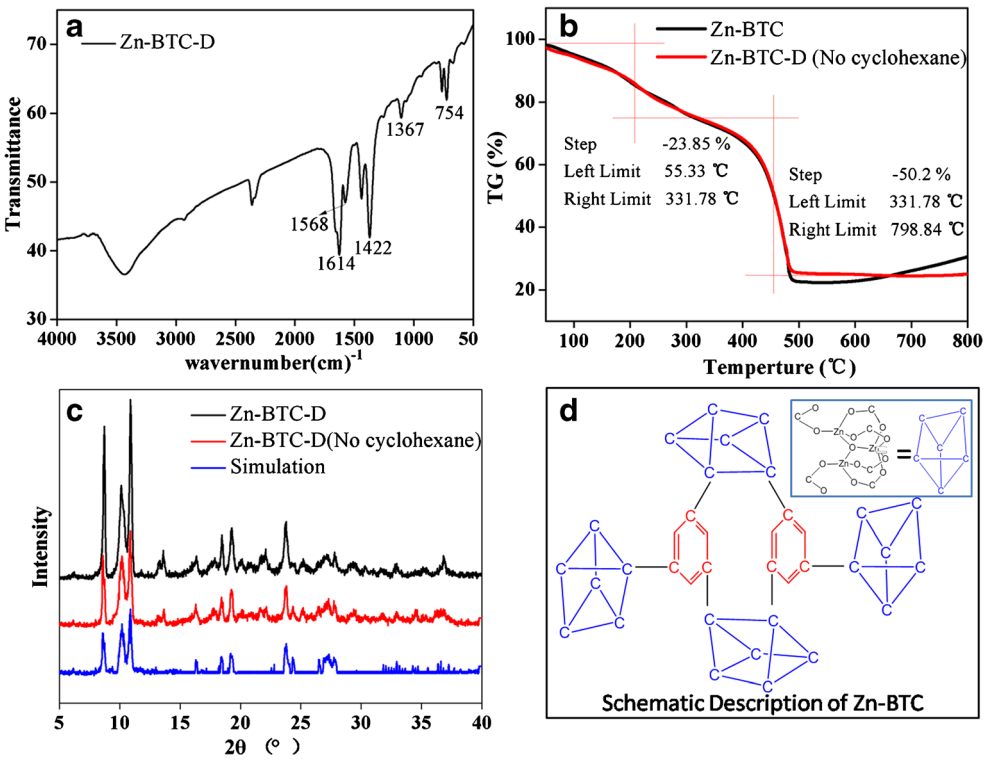

Fig. 1 Characterization of the Zn-BTC-D. **a** FT-IR spectra; **b** TG curve; **c** XRD pattern; **d** Schematic of space structure

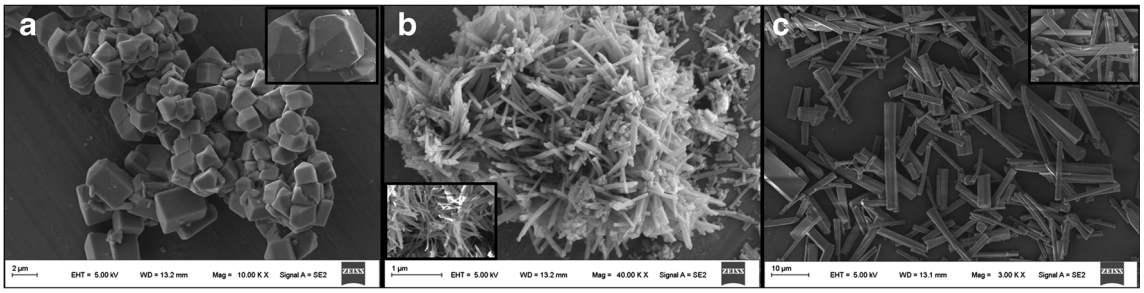

Fig. 2 SEM images of (**a**) Zn-BTC-A; (**b**) Zn-BTC-D; (**c**) Zn-BTC-S

coordinated with Zn. Very broad peak formation at 3100–3600 cm^{-1} in the complex indicate the presence of loosely bound water molecules in Zn-BTC. The most significant peaks are the stretching $V_{C=O}$, V_{C-O} and bending O-H vibrational frequencies seen at 1614, 1568, 1422 and 1367 cm^{-1}, respectively, indicating the presence of a carboxylic acid group.

The TGA curves of Zn-BTC-D and Zn-BTC-D (No cyclohexane) (Fig. 1b) reveal that a gradual weight loss observed at temperatures up to 200 °C for both the crystals is attributed to the evaporation of the solvents that are incorporated into the frameworks, which indicate Zn-BTC-D is stable up to 200 °C. A plateau then follows at temperatures up to 420 °C for two samples. Finally a large weight loss (45%) with a sharp exothermic peak occurs at temperatures between 420 and 500 °C, which are ascribed to the decomposition of the organic components and the crystallization of ZnO.

In order to verify the phase purity of the complexes, powder XRD was performed. As shown in Fig. 1c, samples show diffraction patterns identical to those of the simulated one (Blue line) [23], indicating that the structure of Zn-BTC-D is well preserved and the complexes is pure powder. In the 2θ range of 5.0–40°. The dominant peaks of the synthesized Zn-BTC-D at 8.8°, 10.1°, 10.9°, 13.4°, 16.4°, 18.5°, 19.3°, 23.8°, and the peak positions can be indexed to (111), (200), (220), (222), (400), (331), (420) and (333) [24]. Because of the addition of cyclohexane in this paper, all peaks of Zn-BTC-D (Black line) are all higher than those of Zn-BTC-D (No cyclohexane) (Red line), which indicate the expansion reagent can enhance the crystallinity of the sample.

In order to further demonstrate the space structure of the Zn-BTCD-D, schematic description of inorganic and organic secondary building units including linkers and resulting topologies is shown in Fig. 1d. Zn-BTC-D has structure based on Zn_3O clusters in which each of two Zn centers is bound by two bridging dimonodentate and one monodentate carboxylates. The remaining Zn center is bound by a total of four bridging dimonodentate carboxylates. There are three terminal ligands (two water and one DMF, each bound to different Zn).

To gain a better understanding of the morphological structure of the synthesized Zn-BTC, all samples were also characterized using SEM (Fig. 2). The crystals of Zn-BTC-A grow into well-defined aggregates of tetrahedral and cuboids frameworks approximately 5 μm in size (Fig. 2a). Trigonal prismatic geometry is uncommon for metal ions in extended networks [25], however, using H_3BTC and expansion reagent cyclohexane, we have been able to access this geometry frameworks. From Fig. 2b, the chrysanthemum-like structure of trigonal prisms and triangles of Zn-BTC-D have been assemblied. The long-rod shape of the Zn-BTC-S crystals is clearly seen in the Fig. 2c, the crystal sizes are in the range of 10–20 μm without any aggregation. Some crystals may break in the process of growth due to too long crystal rod. The morphology of Zn-BTC-S samples is consistent with other SEM images published for this similar material [26].

To further characterize the porosity of Zn-BTC, nitrogen adsorption experiments were performed at 77 K. The data of the surface area pore volume and pore size are listed in Table 1. As can be seen in Table 1, all the materials are mesoporous and the BET specific surface area of Zn-BTC MOFs including Zn-BTC-A, Zn-BTC-D, and Zn-BTC-S are

Table 1 Some properties of Zn-BTC for nitrogen adsorption-desorption experiments

Samples	BET surface area ($m^2 \cdot g^{-1}$)	Pore volume [a] ($cm^3 \cdot g^{-1}$)	Pore size [b] (nm)
Zn-BTC-A	12.64	0.13	5.24
Zn-BTC-S	35.08	0.79	9.04
Zn-BTC-D	49.65	0.86	8.40
(No cyclohexan) Zn-BTC-D	55.05	1.54	13.55

[a] Total pore volume

[b] Average pore diameter calculated using BJH method

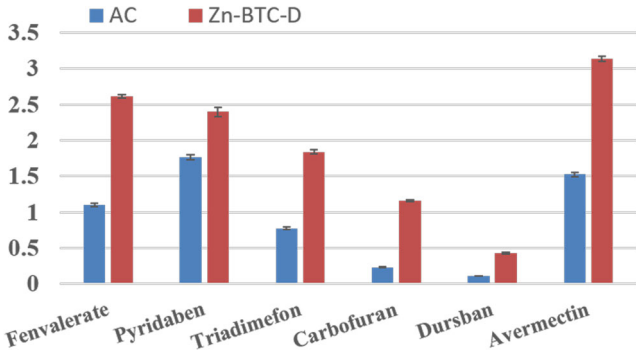

Fig. 3 The adsorption capacity of AC and Zn-BTC-D to six pesticides

measured to be 12.64, 49.65 and 35.08 $m^2 \cdot g^{-1}$, respectively. The pore volume and pore size of Zn-BTC-D is larger than that of Zn-BTC-D (No cyclohexane). This phenomenon can be attributed to the effect of expansion agent, which is consistent with the powder XRD.

Adsorption properties of Zn-BTC

The research about the adsorption characteristics of the Zn-BTC for organic analytes is critical to explore their potential applications. Considering the abundant phenyl rings as bridges throughout the bulk framework of the Zn-BTC, six pesticides including Avermectin, Pyridaben, Dursban, Carbofuran Fenvalerate and Triadimefon were selected as model analyte, and their adsorption affinity on the Zn-BTC-D (In the following experiment, Zn-BTC-D as example) and commercial Active Carbon (AC) as comparision are evaluated and shown in Fig. 3. The relative standard deviations (RSDs) are found to be 1.36–2.17% for AC and 1.12–2.79% for Zn-BTC-D($n = 3$). The six pesticides are compounds with π-π conjugate structure and have strong affinity with Zn-BTC-D rich in aromatic rings. The adsorption amounts of pesticides increased with an increase of the conjugated double bonds and condensed ring, further indicating the potential main role of the π-π stacking interaction. The results suggest that the Zn-BTC-D has unusual potential for removal to pesticides of trace concentrations.

Optimization of method

The following parameters were optimized: (a) Extraction time; (b) Extraction temperature; (c) Amount of adsorbent; (d) Oscillation rate. Respective data and Figures are given in the Electronic Supporting Material (Fig. S1). The following experimental conditions were found to give best results: (a) 30 min was optimized extraction time; (b) The best extraction efficiency was achieved at 25 °C; (c) An amount of 10 mg of adsorbent; (d) 200 rpm was selected in the experiment.

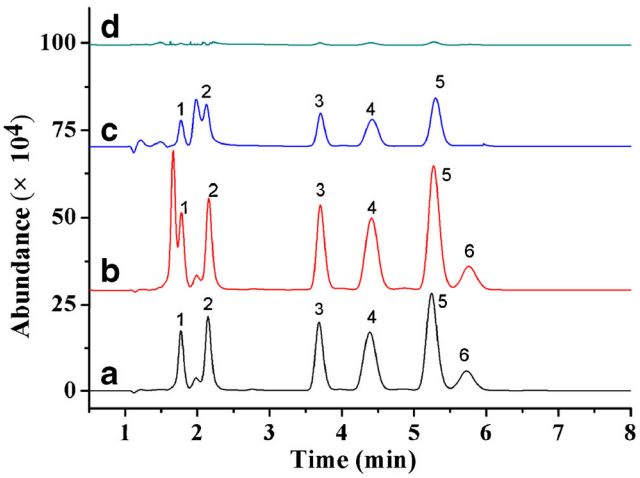

Fig. 4 Chromatograms of six pesticides for the extracts of 50.0 μg L^{-1} standard solution (**a**); industrial wastewater (**b**); domestic sewage (**c**); tap water sample (**d**) with the Zn-BTC-D followed by HPLC/UV analysis. Peaks: 1 Carbofuran, 2 Triadimefon, 3 Dursban, 4 Fenvalerate, 5 Pyridaben, and 6 Avermectin

Validation of method

Optimized DSPE conditions are employed to validate the analytical performance of the method. As shown in Table S2, good linearity with satisfactory squared regression coefficients ($R^2 > 0.9974$) is acquired. The calibration curves for pesticides are linear in the range of 10.0–1000 or 20.0–1000 μg·L^{-1}. The LOD and LOQ are calculated as the concentration corresponding to the signals of 3 and 10 times the standard deviation of the baseline noise, respectively. The LOD and LOQ for seven pesticides are found to be 0.20–1.60 μg·L^{-1} and 0.66–5.28 μg·L^{-1}, respectively, these data are lower than the GB/T5749–2006 (China, Such as Chlorpyrifos ≤20 μg·L^{-1}), which indicate the practicability of the method. The repeatability is measured, and the relative standard deviations (RSDs) are found to be 1.60–9.50% within batch and 3.90–12.2% for batch to batch extraction. These results prove that the Zn-BTC-D is quite stable and

Table 2 An overview reported MOF-based methods for preconcentration of pesticides, insecticides, herbicides and drugs

Analyte	MOF used	Method applied	LODs (μg·L^{-1})	Ref.
Insecticides	MOF-C	DSPE-HPLC-UV	0.34–0.71	[27]
Herbicides	MIL-101	DSPE-HPLC-DAD	0.98–1.90	[28]
Drugs	Polymethacrylate-IL	SPE-HPLC-UV	3.50–7.30	[29]
Pesticides	MOF-Zn	DSPE-HPLC-UV	0.20–1.60	This work

the diffusion method based on chemical bonding is reproducible and reliable.

An overview reported MOF-based methods for preconcentration of pesticides, insecticides, herbicides and drugs is listed in Table 2. The results show that the developed method has lower LODs than the others in the range of 0.34–7.30 $\mu g \cdot L^{-1}$ and can determine more pesticides types. Comparing with the corresponding SPE, the DSPE is rapid, sensitive, cheap, and efficient for the analysis of pesticides in water samples [27–29].

Practical application

To demonstrate the applicability of the investigated Zn-BTC-D, several water samples including East river, West river and tap water were analyzed. As shown in Table S3 and Fig. 4, six pesticides are detected in the industrial wastewater, ranging from 37.3 to16.5 $\mu g \cdot L^{-1}$. No pesticides are found in the tap water, while five pesticides ranging from 13.4 to 33.7 $\mu g \cdot L^{-1}$ are detected in the domestic sewage. The samples are then spiked with standard solutions of pesticides at 20.0 $\mu g \cdot L^{-1}$ to evaluate the recoveries, which ranged from 78.6 to 116.1% for industrial wastewater, 87.5 to 107.9% for domestic sewage, and 97.5 to 101.1% for tap water. The results are owing to the difference of accumulation effect of hazardous pesticides in a different matrix. The nonpolar pesticides are more inclined to transport in complex composition of the sample due to the adsorption of organic matter such as humus and microorganism.

Conclusions

In this study, a novel metal-organic frameworks (MOFs) based on Zinc-benzenetricarboxylates (Zn-BTC) were successfully synthesized using cyclohexane as expansion reagent. The chemical bonding between BTC and Zn endows the MOFs with high chemical stability and desirable durability. Besides that, its successful application as adsorbent in DSPE combined with HPLC-UV was tested by preconcentration of six pesticides in real water samples and showed high sensitivity, unusual adsorption properties, good reproducibility and outstanding selectivity. It will be possible that these Zn-BTC MOFs as supports can be one of the most promising candidates for environmental pollutants separation and enrichment. The structural diversity of MOFs can expand the application scope to related detection schemes.

Acknowledgments This work was generously supported by the Natural Science Foundation of China (No. 21467028, and 21327005), Program for Chang Jiang Scholars and Innovative Research Team, Ministry of Education, China (Grant no. IRT1283), Key Laboratory of Polymer Materials of Gansu Province and Key Laboratory of Ecological Environment Related Polymer Materials of Ministry of Education.

Compliance with ethical standards The author(s) declare that they have no competing interests.

References

1. Chae HK, Siberio-Perez DY, Kim J, Go Y, Eddaoudi M, Matzger AJ, O'Keeffe M, Yaghi OM (2004) A route to high surface area, porosity and inclusion of large molecules in crystals. Nature 427: 523–527
2. Bradshaw D, Garai A, Huo J (2012) Metal-organic framework growth at functional interfaces: thin films and composites for diverse applications. Chem Soc Rev 41:2344–2381
3. Yang XQ, Xia Y (2016) Urea-modified metal-organic framework of type MIL-101(Cr) for the preconcentration of phosphorylated peptides. Microchim Acta 183(7):2235–2240
4. Holman KT (2011) Molecule-constructed microporous materials: long under our noses, increasingly on our tongues and now in our bellies. Angew Chem Int Ed 50:1228–1230
5. Bezzu CG, Helliwell M, Warren JE, Allan DR, McKeown NB (2010) Heme-like coordination chemistry within Nanoporous molecular crystals. Science 327:1627–1630
6. Li QW, Sue CH, Basu S, Shveyd AK, Zhang WY, Barin G, Lei F, Sarjeant AA, Stoddart JF, Yaghi OM (2010) A Catenated strut in a Catenated metal-organic framework. Angew Chem Int Ed 49: 6751–6755
7. Furukawa H, Cordova KE, O'Keeffe M, Yaghi OM (2013) The chemistry and applications metal-organics frameworks. Science 341:1–12
8. Zhang ZJ, Zhao YG, Gong QH, Li Z, Li J (2013) MOFs for CO_2 capture and separation from flue gas mixtures: the effect of multifunctional sites on their adsorption capacity and selectivity. Chem Commun 49:653–611
9. Schoedel A, Scherb C, Bein T (2010) Oriented nanoscale films of metal-organic frameworks by room-temperature gel-layer synthesis. Angew Chem Int Ed 49:7383–7386
10. Carne-Sa´nchez A, Imaz I, Cano-Sarabia M, Maspoch D (2013) A spray-drying strategy for synthesis of nanoscale metalorganic frameworks and their assembly into hollow superstructures. Nat Chem 5:203–211
11. Rocca JD, Liu D, Lin W (2011) Nanoscale metal-organic frameworks for biomedical imaging and drug delivery. Acc Chem Res 44:957–968
12. Safari M, Yamini Y, Masoomi MY, Morsali A, Mani-Varnosfaderani A (2017) Magnetic metal-organic frameworks for the extraction of trace amounts of heavy metal ions prior to their determination by ICP-AES. Microchim Acta 184(4):1–10
13. Song F, Wang C, Falkowski JM, Ma LQ, Lin W (2010) Isoreticular chiral metal-organic frameworks for asymmetric alkene epoxidation: tuning catalytic activity by controlling framework catenation and varying Open Channel sizes. J Am Chem Soc 132:15390–15398
14. Corma A, García H, Llabres I, Xamena FX (2010) Engineering metal organic frameworks for heterogeneous catalysis. Chem Rev 110:4606–4655
15. Ma L, Falkowski JM, Abney C, Lin W (2010) A series of isoreticular chiral metal-organic frameworks as a tunable platform for asymmetric catalysis. Nat Chem 2:838–846
16. Yu HL, Long DY (2016) Highly chemiluminescent metal-organic framework of type MIL-101(Cr) for detection of hydrogen peroxide and pyrophosphate ions. Microchim Acta 183(12):3151–3157
17. Zhang N, Liu XH, Yi R, Shi RR, Gao GH, Qiu GZ (2008) Selective and controlled synthesis of single-crystalline yttrium hydroxide/oxide Nanosheets and nanotubes. J Phys Chem C 112:17788–17795
18. Aziz-Zanjani MO, Mehdinia A (2014) A review on procedures for the preparation of coatings for solid phase microextraction. Microchim Acta 181(11):1169–1190
19. Cho S, Jung SH, Lee KH (2008) Morphology-controlled growth of ZnO nanostructures using microwave irradiation: from basic to complex structures. Phys Chem C 112:12769–12776

20. Inoue S, Fujihara S (2011) Liquid-liquid biphasic synthesis of layered Zinc hydroxides intercalated with long-chain carboxylate ions and their conversion into ZnO nanostructures. Inorg Chem 50: 3605–3612
21. Yu K, Hosono E, Ueno S, Zhou H, Fujihara S (2013) Fabrication of porous cubic architecture of ZnO using Znterephthalate MOFs with characteristic microstructures. Inorg Chem 52:14028–14033
22. Liu C, Li T, Rosi NL (2012) Strain-promoted 'click' modification of a mesoporous metal-organic framework. J Am Chem Soc 134: 18886–18888
23. Chui SSY, Lo SMF, Charmant JPH, Orpen AG, Williams ID (1999) A chemically functionalizable nanoporous material $[Cu_3(TMA)_2(H_2O)_3]$. Science 283:1148–1150
24. Klaus S, Tobias K, Stefan K (2004) Improved synthesis, thermal stability and catalytic properties of the metal-organic framework compound $Cu_3(BTC)_2$. Microporous Mesoporous Mater 73:81–88
25. O'Keeffe M, Hyde BG (1996) Crystal Structures. I. Patterns and symmetry; Mineralogical Society of America, Washington, DC
26. Chen SR, Xue M, Li YQ, Pan Y, Zhu LK, Qiu SL (2015) Porous $ZnCo_2O_4$ nanoparticles derived from a new mixed-metal organic framework for supercapacitors. Inorg Chem Front 2:177–183
27. Liu XL, Wang C, Wan ZC, Wu QH, Wang Z (2015) Nanoporous carbon derived from a metal organic frameworks a new kind of adsorbent for dispersive solid phase extraction of benzoylurea insecticides. Microchim Acta 182:1903–1910
28. Li N, Wang ZB, Zhang LY, Nian L, Lei L, Yang X, Zhang HQ, Yu AM (2014) Liquid-phase extraction coupled with metal-organic frameworks-based dispersive solid phase extraction of herbicides in peanuts. Talanta 128:345–353
29. Wang RL, Yuan YN, Yang X, Han YH, Yan HY (2015) Polymethacrylate microparticles covalently functionalized with an ionic liquid for solid-phase extraction of fluoroquinolone antibiotics. Microchim Acta 182:2201–2208